Biogeosciences, 22, 4491–4505, 2025
https://doi.org/10.5194/bg-22-4491-2025

Biogeosciences Open Access EGU

Burn severity and vegetation type control phosphorus concentration, molecular composition, and mobilization

Morgan E. Barnes[1], J. Alan Roebuck Jr.[2], Samantha Grieger[2], Paul J. Aronstein[3], Vanessa A. Garayburu-Caruso[1], Kathleen Munson[2], Robert P. Young[1,a], Kevin D. Bladon[4], John D. Bailey[4], Emily B. Graham[1,5], Lupita Renteria[1], Peggy A. O'Day[3], Timothy D. Scheibe[1], and Allison N. Myers-Pigg[2,6]

[1]Pacific Northwest National Laboratory, Richland, WA, USA
[2]Pacific Northwest National Laboratory, Sequim, WA, USA
[3]Environmental Systems, University of California – Merced, Merced, CA, USA
[4]College of Forestry, Oregon State University, Corvallis, OR, USA
[5]School of Biological Sciences, Washington State University, Pullman, WA, USA
[6]Department of Environmental Sciences, University of Toledo, Toledo, OH, USA
[a]present address: Washington River Protection Solutions, P.O. Box 850 MSIN M0-01, Richland, WA 99354, USA

Correspondence: Morgan E. Barnes (morgan.barnes@pnnl.gov) and Allison N. Myers-Pigg (allison.myers-pigg@pnnl.gov)

Received: 11 January 2025 – Discussion started: 29 January 2025
Revised: 5 May 2025 – Accepted: 7 May 2025 – Published: 10 September 2025

Abstract. Shifting phosphorus (P) dynamics after wildfires can have cascading impacts from terrestrial to aquatic environments. However, it is unclear whether shifts in P composition or P concentration are responsible for changes in P dynamics post-fire. We used laboratory leaching experiments of Douglas fir forest and sagebrush shrubland chars to examine how the potential mobility of P compounds is influenced by different burn severities. Burning produced a 6.9- and 29-fold increase in particulate P mobilization but a 3.8- and 30.5-fold decrease in aqueous P released for Douglas fir forest and sagebrush shrubland, respectively. The mechanisms driving particulate- and dissolved-phase P compound mobilization were contrasting. Phosphorus compound mobilization in the particulate phase was controlled by solid char total P concentrations, while the aqueous phase was driven by solubility changes of molecular species. Nuclear magnetic resonance (NMR) and X-ray absorption near-edge structure (XANES) on the solid chars indicated that organic orthophosphate monoester and diester species were thermally mineralized to inorganic P moieties with burning in both vegetation types, which decreases P solubility. This coincided with the production of calcium- and magnesium-bound inorganic P compounds. With increasing burn severity there were systematic shifts in P concentration and composition – higher-severity chars mobilized P compounds in the particulate phase, although the magnitude of change was vegetation-specific. Our results indicate a post-fire transformation to both the composition of the solid charred material and how P compounds are mobilized, which may influence its environmental cycling and fate.

1 Introduction

Wildfires are a major modifier of the terrestrial landscape, directly burning around 4 % of the Earth's surface each year (Randerson et al., 2012). They affect both the terrestrial and adjacent aquatic environments and, as such, are considered one of the largest drivers of aquatic impairment (Ball et al., 2021). Organic and inorganic nutrient pools and fluxes can be altered by burning through multiple mechanisms. These include the loss of volatile compounds, altered physiochemical properties from the incomplete combustion of organic material (from partially charred biomass to ash, collectively referred to as chars; Bird et al., 2015), and enhanced material transport from leaching and erosion (Bodí et al., 2014). The degree to which wildfires impact ecosystems, or burn severity, is determined by the extent of organic matter loss or change after fire and is influenced by fire intensity, heating duration, degree of live or dead plant material, and fuel mois-

ture, among other factors (Keeley, 2009). Fire frequency, intensity, severity, and total area burned are expected to increase in many regions, such as the western United States (Doerr and Santín, 2016; Haugo et al., 2019; Jolly et al., 2015). In particular, in the Pacific Northwest, USA, burn severity and total burn area have increased in recent decades (Francis et al., 2023; Halofsky et al., 2020; Reilly et al., 2017; Roebuck et al., 2024). Therefore, it is important to understand the mechanisms behind how wildfires alter nutrient quantity, composition, and mobilization.

Phosphorus (P; occurring primarily as orthophosphate $H_2PO_4^-$, HPO_4^{2-}, or PO_4^{3-}) is an essential element (Smil, 2000) and is often a limiting nutrient to productivity in terrestrial and aquatic environments (Elser et al., 2007). Ecosystem responses post-fire can include shifting terrestrial nutrient acquisition by decreasing phosphatase activity and promoting net primary production (Dijkstra and Adams, 2015; Saa et al., 1993; Vega et al., 2013). Phosphorus-containing compounds transported to aquatic environments can also increase aquatic productivity, influencing invertebrate and fish size and growth rate (Silins et al., 2014). While there is largely agreement across studies that P becomes enriched in chars after wildfire (Butler et al., 2018; Elliott et al., 2013; García-Oliva et al., 2018; Schaller et al., 2015), with increased concentrations in mineral soil (Butler et al., 2018) and river systems following wildfire (Lane et al., 2008; Mishra et al., 2021; Rust et al., 2018), we are lacking a systematic understanding of how variable burning conditions mediate the P concentration of charred organic material and the role of different fire-prone vegetation types (but see Schaller et al., 2015; Wu et al., 2023b; Yusiharni and Gilkes, 2012) in availability for mobilization. Prescribed burns and wildfires occur across a range of burning conditions (Merino et al., 2019; Santín et al., 2018; Vega et al., 2013), which results in a mosaic of post-fire ecosystem responses on the landscape (Keeley, 2009). Therefore, understanding how P biogeochemistry is altered along a burn gradient will provide insights on heterogenous responses observed across burned landscapes.

In the environment, P is found in multiple molecular moieties (i.e., orthophosphate, phosphonate, orthophosphate monoester, orthophosphate diester, polyphosphate; orthophosphate monoester and orthophosphate diester compound classes, referred to as the ester bonds moving forward) which exist in different chemical states (i.e., adsorbed on surfaces, incorporated into minerals, precipitated with metals). Chemical speciation influences the solubility and mobility of P, which in turn impacts its bioavailability (Li and Brett, 2013; Turner et al., 2003b; Weihrauch and Opp, 2018; Yan et al., 2023). For example, bonding energy, or the strength of the bonds, of the chemical species generally increases from organic P to sorbed and mineral-bound P species (Weihrauch and Opp, 2018). The fate of these P species is determined by biological, chemical, physical, and environmental factors, which vary in space and time (Condron et al., 2015; Yan et al., 2023). Thus, the potential influence of wildfire effects on P dynamics and ecosystem productivity cannot be adequately ascertained by only characterizing P concentration. Compared to changes in total P concentration (i.e., the measure of all P compounds), there is less understanding of P molecular composition in charred material and the impact this has on its mobilization (Robinson et al., 2018; Wu et al., 2023a). As such, it is unclear whether P biogeochemical responses post-fire are due to changing composition of the charred material (i.e., composition controlled) and/or an artifact of how P compounds are transported (i.e., mobilized from the solid char to then be transported through the environment). Recent research on laboratory-produced plant-derived chars has demonstrated the use of nuclear magnetic resonance (NMR) to quantify P moiety (Sun et al., 2018; Uchimiya and Hiradate, 2014; Wu et al., 2023b; Xu et al., 2016; Yu et al., 2023) and X-ray absorption near-edge structure (XANES) to identify the chemical state (Robinson et al., 2018; Rose et al., 2019; Wu et al., 2023a; Yu et al., 2023). Taken together, these complementary techniques are useful tools to provide a holistic understanding of P molecular composition and can help to determine the environmental fate, as certain compounds are preferentially volatilized, produced, and transported across the landscape (Son et al., 2015).

Vegetation burn severity is a common metric to describe how wildfires impact ecosystems following a fire, which allows for a post-fire assessment of ecosystem impacts (Keeley, 2009). However, relatively few studies relate burn severity to fire effects on P biogeochemistry (Souza-Alonso et al., 2024; Vega et al., 2013) even though it is a more commonly used field metric than fire intensity because it can be measured after the burn (Zavala et al., 2014). Thus, burn severity allows for field-relevant understanding of burning conditions beyond the impact of temperature alone. Experimental studies along burn severity gradients provide an opportunity to better understand field conditions post-fire. To understand the amount and types of materials derived from plant litter that could be transported from terrestrial to aquatic systems along a burned gradient, we examined how P concentration and molecular composition in solid chars and their leachates vary across a burn severity gradient. We hypothesize that changing P composition in the solid charred materials with increasing burn severity will influence the leachability of P compounds in the particulate and aqueous phases, and this will be moderated by vegetation type. To test this hypothesis and better understand the amount and types of materials that could be mobilized along a burned gradient, we examined how burn severity influences P concentration and molecular composition in experimentally generated solid chars and their leachates from two common vegetation types present in the Pacific Northwest.

2 Materials and methods

All datasets and detailed methodology used in this paper are available from Grieger et al. (Grieger et al., 2022) version 3 and Barnes et al. (Barnes et al., 2024) on the Environmental System Science Data Infrastructure for a Virtual Ecosystem (ESS-DIVE) repository.

2.1 Burn experiments

Vegetation was collected from two fire-prone landscapes of contrasting vegetation types to represent archetypes of vegetation commonly found in the Pacific Northwest, USA, that also have differing wildfire characteristics (Halofsky et al., 2020; Reilly et al., 2017; Roebuck et al., 2024; Stavi, 2019). In this study, we chose to explore vegetation that is representative of Douglas fir forests (*Pseudotsuga menziesii*), which tend to burn in the environment at higher intensities, and sagebrush shrublands (*Artemisia tridentata*), which tend to burn at lower intensities (Stavi, 2019). Samples were chosen to be representative of possible living vegetation and litter materials of the dominant species from these landscapes (Grieger et al., 2022; Myers-Pigg et al., 2024; Roebuck et al., 2024). Exact site locations and sampling details can be found in our accompanying data package (Grieger et al., 2022). For Douglas fir, a mix of living and dead material was collected, while sagebrush was in partial senescence upon collection. All plant materials were air-dried for at least 2 weeks before burning. Woody and canopy materials were mixed at a known ratio (40 % materials < 0.5 cm and 60 % materials > 0.5 cm) before each burn, and this was held constant for each burn (Grieger et al., 2022).

Chars were generated using an open-air burn table, as biochars produced in laboratories have been found to be compositionally different than chars generated in open-air burns and wildfires (Myers-Pigg et al., 2024; Santín et al., 2017). To create burns that would result in a range of vegetation burn severities, we manipulated fire behavior on the burn tables by varying burn temperature, duration of heating, fuel moisture content (by experimentally adding moisture to dried materials), fuel density, and vegetation status (i.e., living or litter). Thermocouples were used to monitor temperature over the burn duration, and char grab samples were targeted for 300 °C, 600 °C, and when flames and smoldering commenced (sagebrush shrubland burns did not reach 600 °C). Char burn severity was visually classified as low, moderate, or high following US Forest Service field metrics based on ash color, degree of consumption, and degree of char (Grieger et al., 2022; Parsons et al., 2010) (Fig. S1 in the Supplement). Thus, burn severity was determined by the extent of organic matter loss or change after fire and is influenced by fire intensity, heating duration, degree of live or dead plant material, and fuel moisture, among other factors and is not a measure of fire intensity (the amount of energy released from a fire) or burn temperature, though it is related to both (Keeley, 2009). The characterization of burn severity results in overlapping maximum temperatures of several of the assigned burn severity categories in our results.

Unburned samples and chars were air-dried; subsamples were finely ground for elemental composition and were stored in the dark at room temperature until further analysis.

2.2 Elemental analysis of solid samples

Total P, sulfur (S), aluminum (Al), iron (Fe), magnesium (Mg), calcium (Ca), sodium (Na), and potassium (K) were measured using an inductively coupled plasma optical emission spectrometer (ICP-OES) model Optima 7300 DV (PerkinElmer, Waltham, MA). Solid samples were digested with aqua regia at 130 °C for 8 h in an incubation oven (ThermoFisher Scientific, Waltham, MA).

For samples that underwent NMR analysis, approximately 0.5 g of finely ground sample was extracted in a 10 mL solution of 0.25 M NaOH and 0.05 M EDTA for 16 h, followed by centrifugation, filtration, and measurement on ICP-OES (Sun et al., 2018; Turner et al., 2003b). The goal of the NaOH-EDTA extraction is to get the maximum amount of P into solution. Extraction efficiencies are reported in Table S1 in the Supplement (see the "Method limitations" section in the Supplement for additional information).

2.3 Solution ^{31}P NMR on solid samples

After aliquoting 3 mL of the NaOH-EDTA extracts for ICP-OES, the remaining supernatants were frozen and lyophilized to concentrate the extracted compounds. Immediately prior to running NMR experiments (Environmental Molecular Science Laboratory; EMSL, Richland, WA), freeze-dried extracts were reconstituted in 0.52 mL deuterium oxide (D_2O) and 0.26 mL of 10 M NaOH, as well as 0.52 mL of a solution containing 0.5 M NaOH and 0.1 M EDTA. Full experimental ^{31}P NMR measurement details are provided in the Supplement. In brief, NMR measurements were conducted on an Agilent DD2 spectrometer operating at a field strength of 14.1 T (242.95 MHz ^{31}P), equipped with a 5 mm Varian broadband direct detect probe. Experiments were conducted at a regulated temperature of 20.0 °C. A standard 1D pulse and acquire experiment was performed using a 90° pulse width and recycle delay equal to $5 \times$ T1, which were calibrated and measured individually for each sample using the orthophosphate peak present in each. Samples were measured for 16 h each with the number of transients acquired dependent upon T1 for each individual sample. Post-acquisition processing and analysis were performed using Mnova 14.0.1 (Mestrelab Research, Spain). Details regarding classification of major P forms, identification of specific P compounds from spiking experiments, quantitation, and method limitations are described in detail in the Supplement (Cade-Menun, 2015; Doolette et al., 2009; Recena et al., 2018) (Fig. S2 in the Supplement).

2.4 Solid-sample P XANES

XANES is a complementary technique to solution ^{31}P NMR because it can discern the complexation environment of P in solid samples (see the "Method limitations" section in the Supplement for additional information). Bulk XANES was conducted on beamline 14-3 at the Stanford Synchrotron Radiation Lightsource (SSRL, Stanford, CA). The beamline was calibrated at the P K edge with the first peak of tetraphenylphosphonium bromide at 2146.96 eV.

Sample spectra were fit using least-squares linear combination in Athena (Ravel and Newville, 2005) (Fig. S3 in the Supplement). Baseline correction and edge-step normalization parameters were varied for individual samples and reference compounds to reduce error (Werner and Prietzel, 2015). Fits were performed with the component sum not forced to unity and a maximum of three reference compounds, and only fits within ±2.5 % were used. If a component fit was less than 5 %, then this reference compound was removed, and the sample was refit with the remaining compounds. The R factor of all sample fits was < 0.05 (Table S2 in the Supplement), indicating a good quality of fit (Kelly et al., 2015). Fits were performed with a variety of Ca, Al, Fe, Mn, K, and Na inorganic and organic P-containing reference compounds. Individual inorganic P (P_i; includes phosphate and pyrophosphate moieties) reference compounds were grouped based on the associated metal, and all organic P compounds (P_o; includes monoester and diester moieties) were kept as a separate category (Fig. S3 and Table S3 in the Supplement). Additional information on sample preparation, linear combination fits, reference compounds, and method limitations is described in the Supplement ("XANES methodology" section).

2.5 Leaching experiments

Leachates from unburned material and char samples were generated in triplicate. Briefly, 25 g of unground sample was shaken in the dark for 24 h in 1000 mL of synthetic rainwater (pH ∼ 5) to simulate what might be mobilized by rain events from the solid material and subsequently transported from terrestrial to aquatic environments (Grieger et al., 2022). Our starting mass was kept constant to understand differences in the amounts of materials leached across burn severity gradients, so our results are directly comparable to temperature gradient studies (Bostick et al., 2018). Therefore, leaching experiments had a different goal of simulating natural mobilization of P compared to the NMR extractions, where we tried to maximize P extracted. Leachates were filtered through a PTFE mesh (2 mm × 0.6 mm) followed by a pre-combusted GF/F filter (< 0.7 µm). Aliquots were immediately taken for subsequent analysis and preserved according to analytical needs described below.

2.6 Elemental analysis of leachates

Coarse filtered (< 2 mm) and < 0.7 µm filtered (i.e., aqueous phase) leachates were preserved in 1 % nitric acid and stored at 4 °C until analysis. Aliquots of 5 mL were transferred to 15 mL centrifuge tubes and acidified to 10 % (v/v) trace metal grade hydrochloric acid and 4 % (v/v) trace metal grade nitric acid. Tubes were fully sealed and heated at 85 °C for 2.5 h in an incubation oven (ThermoFisher Scientific, Waltham, MA), and then total elemental analysis was performed by ICP-OES. Total P of the leachate particulate phase (2 mm to 0.7 µm) was calculated as the difference between the coarse filtered and aqueous phase.

Molybdate reactive P was determined on aqueous-phase leachate aliquots preserved in 0.2 % sulfuric acid and stored at 20 °C, following EPA Method 365.3 (Method 365.3: phosphorus, all forms – colorimetric, ascorbic acid, two reagent). Aqueous non-molybdate reactive P was calculated as the difference between aqueous total P (as measured by ICP-OES) and molybdate reactive P.

2.7 Data analyses

Leachable P (mg per g P; particulate and aqueous phases separately) was calculated by normalizing to the P concentration of the solid samples following Eq. (1) (Fischer et al., 2023).

$$\text{Leachable P}_{\text{particulate or aqueous}} = \frac{\text{leachate P (mg L}^{-1}) \times \text{leaching volume (L)}}{\text{mass of dry char (g)} \times \text{P content of dry char (mg P g}^{-1})} \quad (1)$$

All statistical tests were conducted in R version 4.2.3 (R Core Team, 2023). Data calculations, statistical analyses, and figures are freely available (Barnes et al., 2024). For all statistical analyses, model assumptions were assessed with a Shapiro–Wilk test of normality using the package stats (R Core Team, 2023) and spread-location plots to inspect homoscedasticity. All analyses met assumptions after log transformation. Significance was determined at the $\alpha = 0.05$ level. All data are reported as the mean ± standard deviation unless otherwise stated.

Separate analysis of variance (ANOVA) models were used to test how burn severity, vegetation type, and their interaction influence solid P concentration. For leachate samples (i.e., particulate total P, aqueous total P, aqueous molybdate reactive P), mixed-effect models were run with the same fixed effects as the solid samples and a random effect was used to account for triplicate leachates produced from the same solid sample. Mixed-effect models were performed with the lme4 package (Bates et al., 2015) and were fit by maximum likelihood. Variance inflation factors were used to inspect for multi-collinearity of fixed effects with the car package (Fox and Weisberg, 2018). Post hoc pairwise comparisons were conducted using least-squares means in the emmeans package (Lenth, 2023). These data are presented in box plots, which denote the first and third quartiles as the

lower and upper hinges, while the whiskers are the largest and smallest values up to 1.5 times the interquartile range. Outliers are captured as individual points on the box plots, as they are outside the whiskers.

Path analysis was conducted to analyze the hypothesized relationships that may explain how burn severity and vegetation type influence P compound mobilization (i.e., leachable particulate or aqueous-phase P concentration) indirectly through changes in char conditions (i.e., P concentration and chemical composition). Calcium-bound P_i was used as a proxy for chemical composition because it is a primary control of P compound solubility in charred materials (Schaller et al., 2015; Uchimiya and Hiradate, 2014; Wu et al., 2023b; Yu et al., 2023). Phosphorus compound mobilization was estimated as the average leachable P from the parent solid samples. Models were run with the sem package (Fox, 2006), with burn severity and vegetation type directly impacting the P concentration and proportion of Ca-P_i in the solid samples, which in turn influence the leachable P concentration. Vegetation type is also set up to directly impact burn severity (Fig. S4 in the Supplement).

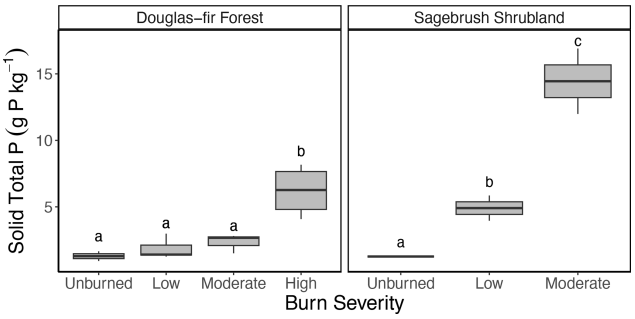

Figure 1. Box plot of P concentration ($g P kg^{-1}$) in the solid samples along Douglas fir forest and sagebrush shrubland burn severity gradients. Letters denote post hoc findings of burn severity significant differences within a vegetation type, where the same lettering indicates no significant difference. See Table 1 for burn duration, temperature, and sample size.

3 Results and discussion

3.1 The magnitude of char P increase with burn severity depends on vegetation type

In our study, using experimental open-air burns, we found that total P concentration (measured using ICP-OES) increased with burn severity in both Douglas fir forest and sagebrush shrubland solid samples (Fig. 1). Our findings were consistent with observations of increasing P concentration from laboratory-produced chars (García-Oliva et al., 2018; Zheng et al., 2013) and in chars collected shortly after wildfire and prescribed burns (Butler et al., 2018). In particular, while our burn treatments did not reach temperatures that would result in P volatilization, they did represent heterogenous burn conditions, incorporating a variety of burn durations and temperature ranges (Grieger et al., 2022; Myers-Pigg et al., 2024) that are consistent with other open-air burn experiments (Brucker et al., 2022, 2024) (Table 1; Fig. S1). The P concentration in unburned Douglas fir forest samples was $1.3 \pm 0.5\,g\,P\,kg^{-1}$ and increased to an average of $6.2 \pm 1.9\,g\,P\,kg^{-1}$ in high-severity burns (ANOVA post hoc $p < 0.001$). On the other hand, unburned sagebrush shrubland material contained $1.3\,g\,P\,kg^{-1}$ compared to $14.5 \pm 3.5\,g\,P\,kg^{-1}$ in the moderate-severity burns (ANOVA post hoc $p < 0.001$), the highest severity classes reached for each vegetation type. The observed increase in char P indicated that retention (i.e., condensation) outweighed loss via volatilization. Generally, P and metal cations volatilize at higher temperatures (774 °C or greater) than carbon (C) and nitrogen (N) (> 200 °C), so they are often retained in charred material rather than lost in gaseous form (Son et al., 2015). Therefore, our study may underestimate P transformations linked to P volatilization from burns that reach higher temperatures than our experimental burns.

Although P concentration in solid samples increased from unburned to the highest burn severity classification reached in both vegetation types, the magnitude was vegetation-dependent (ANOVA interaction term: $F = 6.23$, $p = 0.014$). In Douglas fir forest chars, P concentration was unchanged by burning until high burn severity was reached (post hoc test; low: $p = 0.658$, moderate: $p = 0.277$, high: $p < 0.001$), while P in sagebrush shrubland chars increased even after low burn severity (post hoc test; low: $p = 0.034$, moderate: $p < 0.001$). Post hoc tests further identified the P concentration of sagebrush shrubland chars as significantly greater than Douglas fir forest within the same burn severity classification (low: $p = 0.0038$; moderate: $p < 0.001$), even though unburned samples were not statistically different ($p = 0.962$). On average, total P values in sagebrush shrubland chars were 2.7 and 6.2 times higher than Douglas fir forest in low- and moderate-severity burns, respectively (Fig. 1).

Remarkably, P in moderate-severity sagebrush shrubland chars was even higher than Douglas fir forest high-severity chars; these represent the highest burn severity observed for each vegetation type. Higher maximum char temperature or burn duration does not explain why the P concentration is greater in burned sagebrush shrubland material compared to Douglas fir forest; sagebrush shrublands experienced lower maximum temperatures (530 ± 25 °C) and shorter burn duration (202 ± 3 min) in moderate-severity burns compared to Douglas fir forest high-severity burns (704 ± 78 °C; 783 ± 195 min; Table 1).

One mechanism that could explain such results is that sagebrush shrublands may be composed of volatile organic compounds that are more susceptible to loss compared to Douglas fir forests, leading to selective enrichment of P compounds relative to Douglas fir forest chars. However, emis-

Table 1. Burn characteristics for severity classifications for each vegetation type including mean (standard deviation) duration, low and high range of maximum temperature reached during burn duration, and count of the solid and leachate samples.

Burn severity	Vegetation	Burn duration (min)	Lowest max temp (°C)	Highest max temp (°C)	*n* solids	*n* leachates
Unburned	Douglas fir forest	NA	25	25	2	6
	Sagebrush shrubland	NA	25	25	1	3
Low	Douglas fir forest	342 (403)	295	627	5	15
	Sagebrush shrubland	131 (104)	308	512	2	6
Moderate	Douglas fir forest	456 (303)	589	757	3	9
	Sagebrush shrubland	202 (3)	512	547	2	6
High	Douglas fir forest	783 (195)	589	757	4	12

sion factors and total volatile organic compounds from sagebrush and coniferous fuels are relatively similar (Hatch et al., 2019; McMeeking et al., 2009). This suggests that the observed enrichment of sagebrush shrubland P with burning may be due to differences in the conversion of organic P to inorganic P in the sagebrush shrubland materials, which can arise from different fire conditions (Fiddler et al., 2024). Sagebrush shrublands may be more susceptible to changing P dynamics post-fire because chars are likely enriched in P to a greater extent than Douglas fir forests, even at low severities.

3.2 Solid char molecular composition is influenced by burn severity and vegetation type

Organic P in the solid char was progressively transformed to inorganic species across both vegetation types. Unburned Douglas fir forest and sagebrush shrubland had similar initial percentages of total organic P with 40.5 % ± 3.3 % and 53.7 %, respectively (identified by NMR extracts, Fig. 2; also supported by XANES on solid phase, Fig. 3). As burning progressed, the total organic P pools were reduced to only 12.6 % ± 8.2 % for Douglas fir forest and 10.4 % ± 8.4 % for sagebrush shrubland low-severity chars. While organic P moieties were still present in Douglas fir forest chars produced at moderate severities (4.4 % ± 4.2 %), < 1 % was measured in sagebrush shrubland. Moderate-severity sagebrush shrubland chars more closely resembled high-severity Douglas fir forest, with nearly all organic P moieties lost (< 1 %). This further supports the conclusion that different fire conditions were experienced by Douglas fir forest and sagebrush shrubland in our simulated burns. Although it has been suggested that organic P can be fully transformed to inorganic species at 200 °C (García-Oliva et al., 2018), another study of organic horizons found that organic P moieties persisted after low-, moderate-, and high-severity fires that reached up to 872 °C (Merino et al., 2019). We measured organic P in burns that reached above 600 °C, suggesting that the thermal mineralization of organic to inorganic P compounds is controlled by microscale differences in temperature and selective physical protection (i.e., mineral aggregates) rather than what is observed at overall bulk temperatures and is likely a result of the interaction between temperature, burn duration, and vegetation type experienced by these microsites (Galang et al., 2010; Lopez et al., 2024).

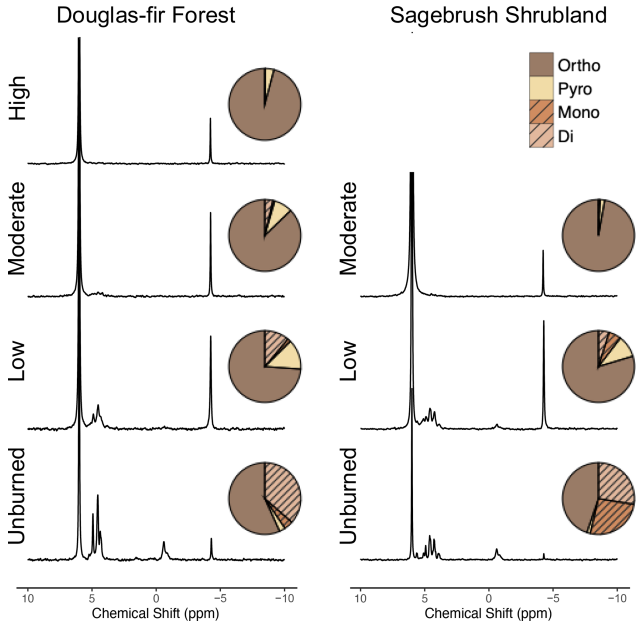

Figure 2. Solution ^{31}P nuclear magnetic resonance (NMR) spectra from a representative solid char sample of each burn severity and vegetation type. The number of scans varied for each sample based on relaxation time, and therefore direct comparisons of peak intensities can only be made within a spectrum (see additional details in the "NMR methods" section in the Supplement). Averaged replicates are represented by pie charts for the proportions of orthophosphate (ortho), pyrophosphate (pyro) monoesters (mono), and diesters (di). Orthophosphate and pyrophosphate are inorganic species (brown colors) and monoester and diesters are organic species (orange colors with hashed lines). See the "NMR methodology" and "Method limitations" sections in the Supplement for additional details and Table 1 for burn duration, temperature, and sample size.

Previous studies have suggested that charred materials containing diester species (two C moieties per P) are more

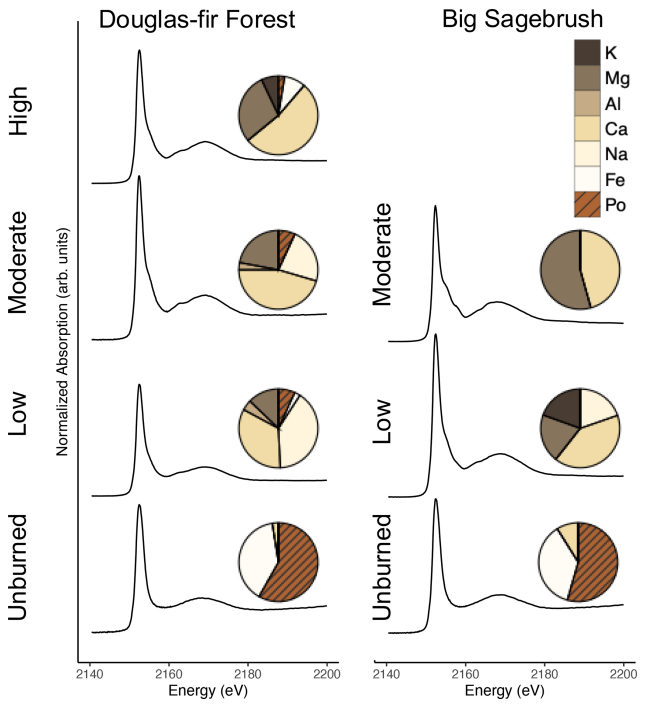

Figure 3. Phosphorus K-edge X-ray absorption near-edge structure (XANES) spectroscopy from a representative solid unburned and char sample of each burn severity and vegetation type. Averaged replicates are represented by pie charts for the proportions of P_i associated with K, Mg, Al, Ca, Na, and Fe (brown colors) and P_o species grouped together regardless of metal association (orange color with hashed lines; see the "XANES methods" section in the Supplement for additional details). See the "XANES methodology" and "Method limitations" sections in the Supplement for additional details and Table 1 for burn duration, temperature, and sample size.

vulnerable to thermal mineralization than monoesters (one C moiety per P) (García-Oliva et al., 2018; Turrion et al., 2010). However, we found that diester and monoester species followed similar proportional decreases in our chars with burning (Fig. S5 in the Supplement). Hence, both readily available (i.e., diester) and less labile (i.e., monoester) organic P species (Condron et al., 2015) were converted to inorganic P at comparable rates, which is similar to forest and shrubland organic horizons subjected to prescribed fire (Merino et al., 2019). This suggests that there is not a fundamental molecular difference in how these moieties respond to burning in organic material such as what is examined in our study, but instead the preferential loss of diesters in burned mineral soil may be because the stronger sorption of monoesters to soil particles attenuates the heat.

Because diester and monoester species were lost at similar proportions, the composition of the unburned material dictated the resulting char P composition and potential bioavailability. Across both vegetation types, we identified phospholipids, DNA, RNA (diester region), phytate, and sugar phosphates (monoester region; Fig. 2; Table S4 in the Supplement), which follows other studies of vegetation P composition (Doolette and Smernik, 2016; Noack et al., 2012). However, the proportions of these species were vegetation-dependent, where unburned Douglas fir forest was dominated by diesters (36.5 % ± 9.1 %) with minor percentages of monoesters (4.1 % ± 5.7 %), whereas sagebrush shrubland was nearly equal parts diesters (27.6 %) and monoesters (26.1 %). RNA, DNA, phospholipids, and sugar phosphates are considered bioavailable due to their weak adsorption, whereas phytate strongly sorbs to both organic and inorganic particles, making it relatively less available for biological uptake (Condron et al., 2015; Li and Brett, 2013; Turner et al., 2003a). Douglas fir forest was composed of a greater proportion of these bioavailable organic species in unburned (36.8 % ± 7.6 %) and low-severity burns (12.4 % ± 8.4 %) compared to sagebrush shrubland (unburned: 32.4; low: 8.0 % ± 4.5 %).

With increased burn severity, Douglas fir forest (high-severity) and sagebrush shrubland (moderate-severity) organic speciation converged with only < 1 % of organic P (as RNA) remaining. Prior studies using NMR in plant-based biochar produced from 300–800 °C found that char was composed of entirely inorganic P, including orthophosphate (27 %–97 %) and pyrophosphate (3 %–71 %; although one sample produced at 350 °C was 2 % phospholipids) (Sun et al., 2018; Uchimiya et al., 2015; Uchimiya and Hiradate, 2014). The unburned parent material in these studies had variable starting compositions with organic P ranging from 3 %–87 % (as phytate). The extent of organic P loss in these studies is most similar to our higher-severity samples, once again demonstrating that factors beyond just temperature determine the composition of P in charred material. Overall, these findings suggest that organic P moieties in charred material are determined by the degree of burning, where lower-severity chars resemble the starting composition, and this is influenced by vegetation type.

As organic species were thermally mineralized in our chars, inorganic P, such as pyrophosphate, was produced (Fig. 2). Pyrophosphate can be produced either from orthophosphate or phytate and is thought to largely originate from fungal tissue (Bünemann et al., 2008; Makarov et al., 2005), although it has been found in some plants (Noack et al., 2012; Wu et al., 2023b). We found that pyrophosphate peaked in low-severity chars across both vegetation types, reaching 13.6 % ± 3.1 % in Douglas fir forest and 9.9 % ± 6.2 % in sagebrush shrubland burns. Prior NMR studies on plant chars produced between 350–800 °C have also observed an increase in the proportion of pyrophosphate relative to unburned material, followed by a decrease at higher charring conditions (Sun et al., 2018; Uchimiya and Hiradate, 2014). Variability in pyrophosphate from naturally produced chars has also been observed. For example, post-wildfire, pyrophosphate was ∼ 3 % in a pine forest (García-Oliva et al., 2018), absent in a eucalyptus forest (Santín et al., 2018), 0 %–13 % of cedar–hemlock forests (Cade-Menun

et al., 2000), and 3 %–7 % from pine forests and shrublands (Merino et al., 2019). Thus burned organic material, especially in chars produced in low-severity wildfire and prescribed burns, may be an important, yet underappreciated, source of pyrophosphate in the environment.

The production of pyrophosphate in our charred plant material is likely a result of the initial organic matter composition and burning conditions (Wu et al., 2023b; Yu et al., 2023). Pyrophosphate and other polyphosphates can be produced from orthophosphate during burning, with the thermal degradation of phytate (organic P; monoester) contributing more orthophosphate (Robinson et al., 2018; Rose et al., 2019; Uchimiya and Hiradate, 2014). Pyrophosphate was greater in Douglas fir forest chars compared to sagebrush shrublands, even though sagebrush shrubland chars contained more phytate in the unburned material (Fig. 2). This indicates that pyrophosphate was primarily produced from polymerization and dehydration of orthophosphate, and not from thermal degradation of phytate in our chars (Uchimiya and Hiradate, 2014).

Although pyrophosphate peaked in low-severity chars, we found that the percentage of total inorganic P species continued to increase with burning across both vegetation types, as measured by NMR on solid extracts and XANES of intact solid samples (Figs. 2 and 3; Tables S2 and S4), demonstrating additional transformations to P composition with increasing severity. Inorganic species, measured by XANES, in unburned material were composed largely of P compounds associated with Fe (37 % sagebrush shrubland; 40 % ± 5 % Douglas fir forest; fitting primarily as P_i sorbed to the surface of goethite) and a minor component of Ca-bound P_i species (3 % ± 3 % Douglas fir forest; 9 % sagebrush shrubland; fitting mostly as apatite). The proportion of Ca- and Mg-P_i (fitting as magnesium phosphate and/or struvite) increased with burn severity (Fig. 3; Table S2). Douglas fir forest high-severity chars had 52.8 % ± 8.3 % Ca-P_i and 29.0 % ± 9.9 % Mg-P_i, while sagebrush shrubland moderate-severity chars contained 45.1 % ± 0.1 % Ca-P_i and 53.7 % ± 0.1 % Mg-P_i.

Other studies using XANES support the production of Ca-P_i, along with Fe- or Mg-P_i in plant-based chars and ash (Robinson et al., 2018; Sun et al., 2018; Uchimiya and Hiradate, 2014; Wu et al., 2023a), whereas studies using other techniques (solid-state NMR, sequential fractionation) have found that higher temperatures result in greater Ca- and Al-P_i (García-Oliva et al., 2018; Xu et al., 2016). Hydroxyapatite and other stable forms of Ca-P_i minerals are known to be produced by organic matter combustion (Uchimiya and Hiradate, 2014), so it follows that these P species are produced with burning and progressively increase along our burn severity gradient. P compound bonding environments have been found to resemble stoichiometric ratios of the burned material (Wu et al., 2023a; Zwetsloot et al., 2015). Our findings support this, where Ca- and Mg-P_i species increased as the proportion of Ca and Mg also increased (Fig. 3; Tables S2, S5, and S6 in the Supplement). Phosphorus mobility and bioavailability of P compounds are likely influenced by increased inorganic P proportions because Ca-P_i, especially apatite, is considered to have low water extractability and apparent bioavailability (García-Oliva et al., 2018; Li and Brett, 2013; Zwetsloot et al., 2015).

3.3 Leachable particulate- and aqueous-bound P have contrasting mobilization patterns with burning and are under differing controls

As burn severity increased, the enriched P of the solid chars resulted in greater particulate P mobilized (assessed via leaching experiments), regardless of vegetation type ($\beta = 0.78$, $p < 0.001$, $r^2 = 0.68$; Figs. 4 and 5). Burning resulted in a 6.9- and 29-fold increase in particulate P mobilization from Douglas fir forest (high-severity) and sagebrush shrubland (moderate-severity) chars, respectively (Fig. 4). Phosphorus compounds may be largely physically protected in the matrix of the charred material (70 %–90 % residual P in sequential fractionation scheme, Wu et al., 2023b), and therefore it follows that particulate P patterns are controlled by changes in solid char concentration; charred material becomes enriched with P and there is production of highly mobile particulates (such as ash; Blake et al., 2010). Path analysis identified burn severity ($\beta = 0.61$, $p < 0.001$) and vegetation type ($\beta = 0.65$, $p < 0.001$) as having direct influence on solid char P concentration ($r^2 = 0.64$; Fig. 5). Mixed-effect model results further demonstrate that the effect burn severity has on leachable particulate P is vegetation-dependent (interaction term of mixed-effect model; $p = 0.009$). Moderate-severity sagebrush shrubland chars mobilized 5.2 times more P in the particulate phase than Douglas fir forest ($p = 0.04$). Particulate P mobilized from charred material can be transported to waterways, as a meta-analysis found that unfiltered P concentrations in the western United States increased ~ 1.7 times after wildfire ($n = 46$) (Rust et al., 2018).

In contrast to leachable particulate P, mobilization of P in the aqueous phase decreased 3.8-fold for Douglas fir forest and 30.5-fold for sagebrush shrubland with burning (Fig. 4). Prior work from laboratory-produced plant chars has found decreased water-soluble P even though solid char concentration increased with burning (Gundale and DeLuca, 2006; Mukherjee and Zimmerman, 2013; Wu et al., 2011; Yu et al., 2023; Zheng et al., 2013). Instead of being concentration-controlled like particulate P, aqueous P mobilization was composition-controlled (represented as percentage of Ca-P_i in our path analysis, $\beta = -0.44$, $p = 0.041$, $r^2 = 0.34$; Fig. 5). We chose to represent P composition in the path analysis as Ca-P_i to simplify the path analysis interpretation. In reality, drivers of aqueous P mobilization extend beyond Ca-P_i and include other compositional shifts, such as Mg-P_i, organic P speciation, and pH. Phosphorus compound adsorption to multivalent cations (Ca^{2+}, Mg^{2+}, Fe^{3+}, and Al^{3+}) can decrease aqueous-phase export (Glaser et al., 2002). Indeed, we found that higher-severity burns had greater con-

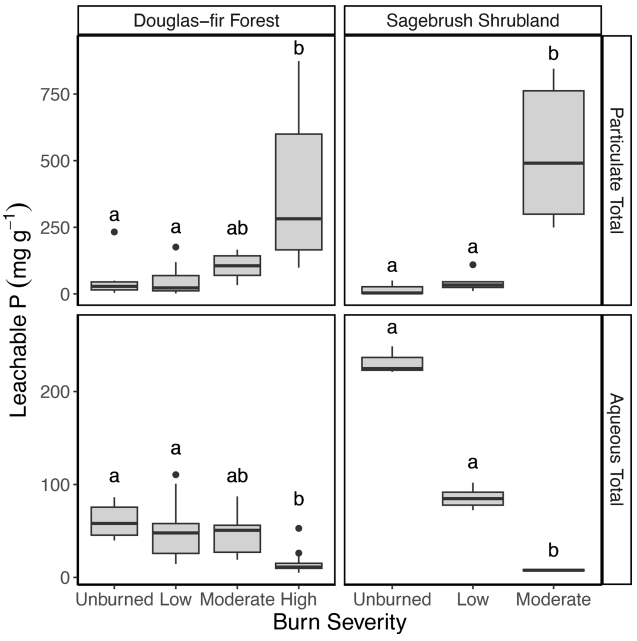

Figure 4. Box plot of the relationship between burn severity and vegetation type with leachable P concentration ($mg\,P\,g^{-1}$; calculated from Eq. 1) for total P in the particulate phase and total P in the aqueous phase. Molybdate reactive P in the aqueous phase is reported in the Supplement. Letters denote post hoc findings of burn severity significant differences within a vegetation type, where the same lettering indicates no significant difference. Note the difference scales of the *y* axis for the particulate and aqueous phases. See Table 1 for burn duration, temperature, and sample size and Fig. S6 in the Supplement for leachable aqueous molybdate reactive P results.

centrations of metals (Tables S5 and S6), which interacted with P to form primarily Ca- and Mg-P_i species (Fig. 3; Table S2).

Additional changes to char composition, including organic P speciation and pH, also likely contributed to decreased aqueous P mobilization with increased burning. We found a decrease in non-molybdate reactive aqueous P, which is largely composed of organic P species (Condron et al., 2015), with increasing burn severity (mixed-effect model interaction term: $p < 0.001$, Fig. S6), indicating less mobilization of organic P species with burning. The quantity of mobilized P compounds from char is also related to pH (Fig. 6), where fewer P compounds are released at higher pH (Silber et al., 2010; Zheng et al., 2013). We found that aqueous P mobilization had an inverse relationship with pH for both Douglas fir forest ($p < 0.001$; $r^2 = 0.45$) and sagebrush shrubland ($p < 0.001$, $r^2 = 0.97$; Fig. 6). Overall, changing chemical composition of the charred material decreases solubility and therefore reduces aqueous P mobilization into the environment (Robinson et al., 2018; Uchimiya et al., 2015; Wu et al., 2023b; Xu et al., 2016).

The extent of decreased aqueous P mobilization was vegetation-dependent (interaction term of mixed-effect model; $p < 0.001$; Fig. 4). However, because both vegetation types had similar percentages of Ca-P_i ($p = 0.18$; $r^2 = 0.15$), it indicates additional controls on aqueous P mobilization. In addition to Ca-P_i and Mg-P_i, moderate-severity Douglas fir forest contained P compounds associated with Na (XANES: $22.7\,\% \pm 22.1\,\%$) and organic P species (XANES: $6.9\,\% \pm 11.9\,\%$; NMR: $4.4\,\% \pm 4.2\,\%$), whereas Na-P_i was not detected in sagebrush shrubland and organic P was $< 1\,\%$ (XANES: $0\,\% \pm 0\,\%$; NMR: $0.7\,\% \pm 0.4\,\%$; Figs. 2 and 3; Tables S2 and S4). Greater solubility of these chemical species likely contributes to Douglas fir forest moderate-severity burns mobilizing 6.4 times more aqueous P than sagebrush shrubland ($p = 0.004$). Changing chemical speciation from soluble organic and inorganic P to less soluble inorganic species (Li and Brett, 2013; Mukherjee and Zimmerman, 2013; Xu et al., 2016) resulted in the decreased export of P compounds with increased burn severity and contributed to the quantity of P compounds mobilized from the respective vegetation types. This has important implications for P compounds that are transported in the environment because organic P can leach faster than many inorganic compounds (McDowell et al., 2021) and Na-P_i has been found to have high nutrient uptake and bioavailability (Li and Brett, 2013).

4 Conclusions

We found systematic changes in P chemistry across vegetation types; with increasing burn severity there were systematic shifts in P concentration and composition. We summarize our findings into a conceptual model to synthesize the main findings from this study (Fig. 7). From unburned to high severity, identifiable structures decreased with increasing black charring and/or white ash (Fig. 7 panel 1; Fig. S1). Total Ca, Fe, Al, K, Ma, and Na concentrations increased (Table S5). Solid char concentration and composition controlled how P compounds were mobilized from burned material. Overall, burning resulted in an increase in char P concentration (Fig. 7 panel 1), which subsequently controlled the mobilization of particulate-bound P compounds from the chars. As burning progressed, chars compositionally transitioned from proportionally more organic P species, including both monoester and diesters, to Ca- and Mg-bound inorganic P species (Fig. 7 panel 1). These compositional changes resulted in fewer soluble inorganic P species and therefore reduced aqueous P mobilization in higher-severity burns (Fig. 7 panel 2). Across vegetation types, chars became more divergent from the unburned vegetation material in P composition and mobilization potential as burning continued. Burn severity and vegetation type indirectly influenced the quantity and leachable phase (i.e., particulate or aqueous) of P compounds that were mobilized from charred material by altering solid sample concentration and composition.

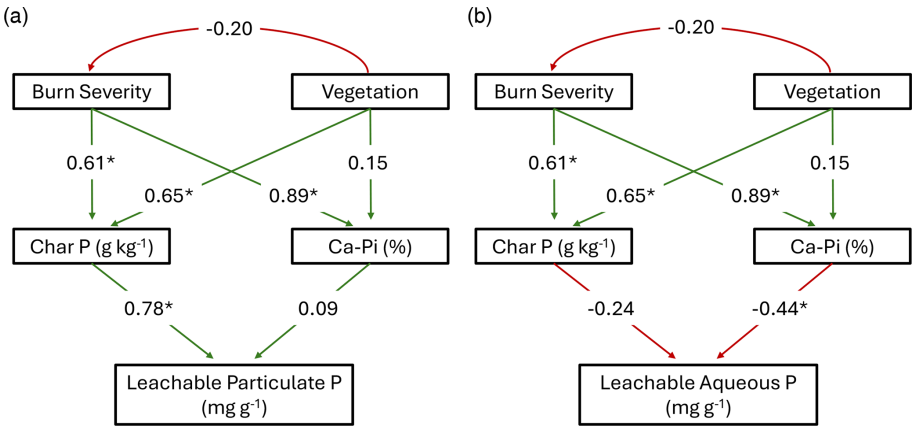

Figure 5. Path analysis model results for the impact of burn severity and vegetation type on leachable P in the **(a)** particulate and **(b)** aqueous phases, as mediated by solid unburned and char P concentration and chemical composition. All relationships are reported with significance ($\alpha = 0.05$) denoted by an asterisk symbol on the standardized correlation coefficient (analogous to relative regression weights). Paths are green for positive relationships and red for negative. Leachable particulate P model: $\chi^2 = 16.277$, $p < 0.05$, $df = 3$, RMSEA = 0.483, AIC = 108.3; leachable aqueous P model: $\chi^2 = 19.032$, $p < 0.05$, $df = 3$, RMSEA = 0.530, AIC = 122.1. See Fig. S4 for the original hypothesized model.

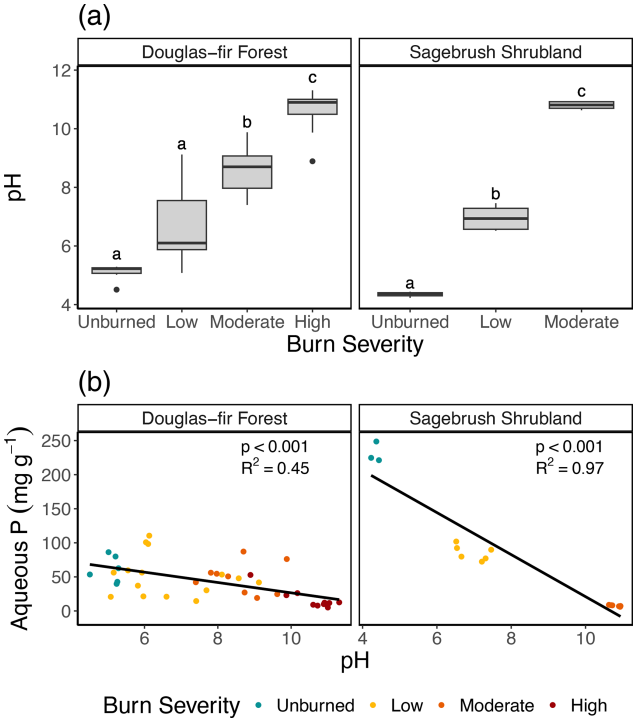

Figure 6. **(a)** Box plot of pH and burn severity. Letters denote post hoc findings of burn severity significant differences within a vegetation type, where the same lettering indicates no significant difference. See Table 1 for burn duration, temperature, and sample size. **(b)** Relationship between pH and aqueous P for Douglas fir forest and sagebrush shrubland.

Although both vegetation types followed similar concentration and compositional patterns, sagebrush shrubland had greater P transformations than Douglas fir forest across our P burn severity conceptual model (Figs. 7 and S4). The P concentrations of Douglas fir forest chars and leachates were more resilient to change with burning compared to sagebrush shrubland. Phosphorus transformations in sagebrush shrubland moderate-severity burns generally chemically resembled that of Douglas fir forest high-severity burns (i.e., higher solid P concentrations, more particulate leachable P, and more inorganic P). Taken together, this indicates that although sagebrush shrubland experiences more low- and moderate-severity burns than Douglas fir forests (Stavi, 2019), the response of P chemistry in the environment post-fire may resemble Douglas fir forests burned at higher severities. This response is important to note as shifts in fire severity do not occur uniformly across all ecosystem types (Francis et al., 2023; Halofsky et al., 2020; Reilly et al., 2017), which may influence post-fire P dynamics across ecosystems.

The ultimate fate of P in the environment is determined by the interactions among biological, chemical, physical, and environmental factors (Condron et al., 2015; Yan et al., 2023). Our leaching experiments provide insight into the potential mobilization mechanisms of P release from solid vegetation chars. The key to bioavailable P is that it can enter solution for subsequent uptake by plants and microbes (Kruse et al., 2015). We found that burning resulted in less P released into the environment in the aqueous phase; therefore, the differences in aqueous P we observed with burn severity can influence the biogeochemical cycling of P by altering its availability for biological uptake and physical transport. The increase in particulate-bound P may be an important

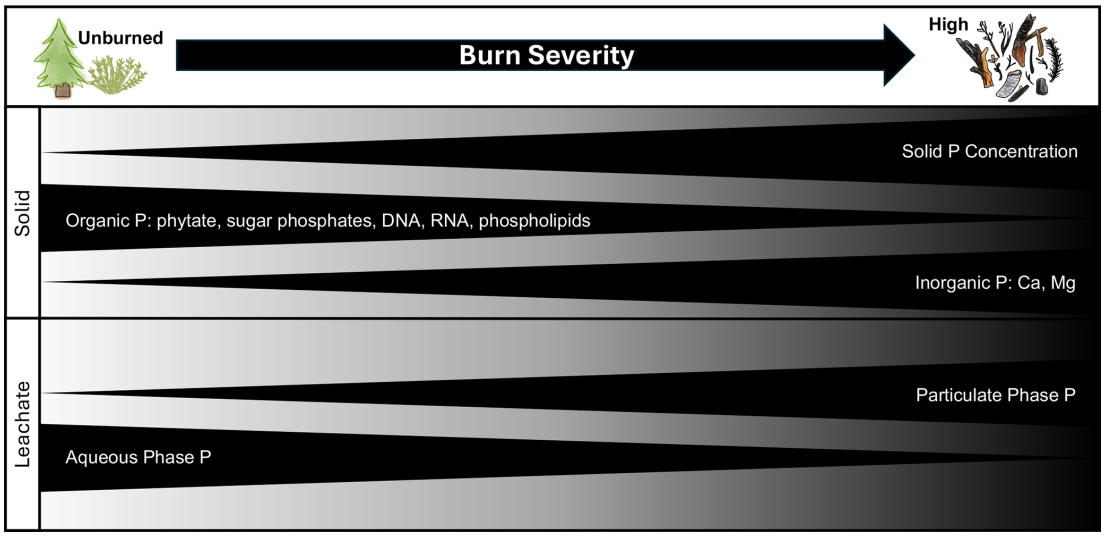

Figure 7. Conceptual framework for phosphorus biogeochemical shifts with increasing burn severity where solid P concentration increases and organic P species decrease while inorganic P increases. Leachates from the solid samples increased in the mobilization of P in the particulate phase but decreased in aqueous P with burning.

source of available P over longer time frames compared to starting vegetation. For instance, P mobilization into riverine systems can be long-lived following fire, altering P budgets and aquatic ecosystem health (Bodí et al., 2014; Emmerton et al., 2020; Rust et al., 2018; Santín et al., 2018; Silins et al., 2014). Our study helps to provide additional information on the potential environmental fate of P post-fire in the context of different burn severities and ecosystem types.

Code and data availability. All data and code are publicly available on the Environmental System Science Data Infrastructure for a Virtual Ecosystem (ESS-DIVE) repository (https://doi.org/10.15485/2547035, Barnes et al., 2024; https://doi.org/10.15485/1894135, Grieger et al., 2022).

Supplement. The supplement related to this article is available online at https://doi.org/10.5194/bg-22-4491-2025-supplement.

Author contributions. Conceptualization: MEB, ANMP, JAR Jr., KDB, EBG, SG, TDS. Methodology and software: ANMP, MEB, SG, JDB, KDB, EBG, PJA, VAGC, KM, JAR Jr., RPY, PAO'D, LR. Investigation: MEB, PJA, SG, KM, LR, JAR Jr., JDB, KDB, RPY. Data curation: MEB, SG, PJA, VAGC, ANMP, KM, JDB, KDB, LR, JAR Jr. Formal analysis: MEB, ANMP, JAR Jr., VAGC, PJA, PAO'D, RPY. Validation: MEB, PJA, KM, VAGC, ANMP, PAO'D, RPY. Visualization: MEB, ANMP, SG. Writing (original draft): MEB, ANMP, JAR Jr., SG, KM, RPY. Writing (review and editing): MEB, PJA, JDB, KDB, VAGC, EBG, ANMP, PAO'D, LR, JAR Jr., TDS, RPY.

Competing interests. The contact author has declared that none of the authors has any competing interests.

Disclaimer. Publisher's note: Copernicus Publications remains neutral with regard to jurisdictional claims made in the text, published maps, institutional affiliations, or any other geographical representation in this paper. While Copernicus Publications makes every effort to include appropriate place names, the final responsibility lies with the authors.

Acknowledgement. We thank Christopher Myers for his assistance with the ICP analyses and Sophia McKever for help with measuring molybdate reactive P. This research was supported by the U.S. Department of Energy, Office of Science, Office of Biological and Environmental Research, Environmental System Science (ESS) Program. This contribution originates from the River Corridor Scientific Focus Area project at Pacific Northwest National Laboratory (PNNL). PNNL is operated by Battelle Memorial Institute for the United States Department of Energy under contract no. DE-AC05-76RL01830. Portions of this research were performed on a project award (https://doi.org/10.46936/lser.proj.2021.51840/60000342) from the Environmental Molecular Science Laboratory (EMSL) (grid.436923.9), a DOE Office of Science User Facility sponsored by the Biological and Environmental Research program under contract no. DE-AC05-76RL01830. XANES data were collected from the Stanford Synchrotron Radiation Lightsource, SLAC National Accelerator Laboratory, which is supported by the US Department of Energy, Office of Science, Office of Basic Energy Sciences under contract no. DE-AC02-76SF00515. We would like to give special thanks to Erik Nelson, the beamline scientist from SSRL who helped us collect those data.

Financial support. This research has been supported by the U.S. Department of Energy, Office of Science, Office of Biological and Environmental Research, Environmental System Science (ESS) program (grant no. 54737).

Review statement. This paper was edited by David McLagan and reviewed by two anonymous referees.

References

Ball, G., Regier, P., González-Pinzón, R., Reale, J., and Van Horn, D.: Wildfires increasingly impact western US fluvial networks, Nat. Commun., 12, 2484, https://doi.org/10.1038/s41467-021-22747-3, 2021.

Barnes, M. E., Aronstein, P. J., Bailey, J. D., Bladon, K. D., Forbes, B., Garayburu-Caruso, V. A., Grieger, S., Graham, E. B., McKever, S. A., Myers, C. R., Munson, K. M., O'Day, P. A., Powers-McCormack, B., Renteria, L., Roebuck, A., Scheibe, T. D., Young, R. P., and Myers-Pigg, A. N.: Data and scripts associated with: "Burn severity and vegetation type control phosphorus concentration, molecular composition, and mobilization", ESS-Dive [data set], https://doi.org/10.15485/2547035, 2024.

Bates, D., Mächler, M., Bolker, B., and Walker, S.: Fitting Linear Mixed-Effects Models Using lme4, J. Stat. Softw., 67, 1–48, 2015.

Bird, M. I., Wynn, J. G., Saiz, G., Wurster, C. M., and McBeath, A.: The pyrogenic carbon cycle, Annu. Rev. Earth Pl. Sc., 43, 273–298, 2015.

Blake, W. H., Theocharopoulos, S. P., Skoulikidis, N., Clark, P., Tountas, P., Hartley, R., and Amaxidis, Y.: Wildfire impacts on hillslope sediment and phosphorus yields, J. Soil. Sediment., 10, 671–682, 2010.

Bodí, M. B., Martin, D. A., Balfour, V. N., Santín, C., Doerr, S. H., Pereira, P., Cerdà, A., and Mataix-Solera, J.: Wildland fire ash: Production, composition and eco-hydro-geomorphic effects, Earth-Sci. Rev., 130, 103–127, 2014.

Bostick, K. W., Zimmerman, A. R., Wozniak, A. S., Mitra, S., and Hatcher, P. G.: Production and Composition of Pyrogenic Dissolved Organic Matter From a Logical Series of Laboratory-Generated Chars, Front. Earth Sci., 6, 43, https://doi.org/10.3389/feart.2018.00043, 2018.

Brucker, C. P., Livneh, B., Minear, J. T., and Rosario-Ortiz, F. L.: A review of simulation experiment techniques used to analyze wildfire effects on water quality and supply, Environ. Sci.-Proc. Imp., 24, 1110–1132, 2022.

Brucker, C. P., Livneh, B., Butler, C. E., and Rosario-Ortiz, F. L.: A laboratory-scale simulation framework for analysing wildfire hydrologic and water quality effects, Int. J. Wildland Fire, 33, WF23050, https://doi.org/10.1071/wf23050, 2024.

Bünemann, E. K., Smernik, R. J., Marschner, P., and McNeill, A. M.: Microbial synthesis of organic and condensed forms of phosphorus in acid and calcareous soils, Soil Biol. Biochem., 40, 932–946, 2008.

Butler, O. M., Elser, J. J., Lewis, T., Mackey, B., and Chen, C.: The phosphorus-rich signature of fire in the soil-plant system: a global meta-analysis, Ecol. Lett., 21, 335–344, 2018.

Cade-Menun, B. J.: Improved peak identification in ^{31}P-NMR spectra of environmental samples with a standardized method and peak library, Geoderma, 257–258, 102–114, 2015.

Cade-Menun, B. J., Berch, S. M., Preston, C. M., and Lavkulich, L. M.: Phosphorus forms and related soil chemistry of Podzolic soils on northern Vancouver Island. II. The effects of clear-cutting and burning, Can. J. Forest Res., 30, 1726–1741, 2000.

Condron, L. M., Turner, B. L., and Cade-Menun, B. J.: Chemistry and dynamics of soil organic phosphorus, in: Phosphorus: Agriculture and the Environment, (Eds.) J. T. Sims and A. N. Sharpley, American Society of Agronomy, Crop Science Society of America, and Soil Science Society of America, Madison, WI, USA, 87–121, 2015.

Dijkstra, F. A. and Adams, M. A.: Fire Eases Imbalances of Nitrogen and Phosphorus in Woody Plants, Ecosystems, 18, 769–779, 2015.

Doerr, S. H. and Santín, C.: Global trends in wildfire and its impacts: perceptions versus realities in a changing world, Philos. T. Roy. Soc. B, 371, 20150345, https://doi.org/10.1098/rstb.2015.0345, 2016.

Doolette, A. L. and Smernik, R. J.: Phosphorus speciation of dormant grapevine (*Vitis vinifera* L.) canes in the Barossa Valley, South Australia, Aust. J. Grape Wine R., 22, 462–468, 2016.

Doolette, A. L., Smernik, R. J., and Dougherty, W. J.: Spiking improved solution phosphorus-31 nuclear magnetic resonance identification of soil phosphorus compounds, Soil Sci. Soc. Am. J., 73, 919–927, 2009.

Elliott, K. J., Knoepp, J. D., Vose, J. M., and Jackson, W. A.: Interacting effects of wildfire severity and liming on nutrient cycling in a southern Appalachian wilderness area, Plant Soil, 366, 165–183, 2013.

Elser, J. J., Bracken, M. E. S., Cleland, E. E., Gruner, D. S., Harpole, W. S., Hillebrand, H., Ngai, J. T., Seabloom, E. W., Shurin, J. B., and Smith, J. E.: Global analysis of nitrogen and phosphorus limitation of primary producers in freshwater, marine and terrestrial ecosystems, Ecol. Lett., 10, 1135–1142, 2007.

Emmerton, C. A., Cooke, C. A., Hustins, S., Silins, U., Emelko, M. B., Lewis, T., Kruk, M. K., Taube, N., Zhu, D., Jackson, B., Stone, M., Kerr, J. G., and Orwin, J. F.: Severe western Canadian wildfire affects water quality even at large basin scales, Water Res., 183, 116071, https://doi.org/10.1038/s41467-021-22747-3, 2020.

Fiddler, M. N., Thompson, C., Pokhrel, R. P., Majluf, F., Canagaratna, M., Fortner, E. C., Daube, C., Roscioli, J. R., Yacovitch, T. I., Herndon, S. C., and Bililign, S.: Emission factors from wildfires in the Western US: An investigation of burning state, ground versus air, and diurnal dependencies during the FIREX-AQ 2019 campaign, J. Geophys. Res., 129, e2022JD038460, https://doi.org/10.1029/2022jd038460, 2024.

Fischer, S. J., Fegel, T. S., Wilkerson, P. J., Rivera, L., Rhoades, C. C., and Rosario-Ortiz, F. L.: Fluorescence and Absorbance Indices for Dissolved Organic Matter from Wildfire Ash and Burned Watersheds, ACS EST Water, 3, 2199–2209, 2023.

Fox, J.: Teacher's Corner: Structural Equation Modeling With the sem Package in R, Struct. Equ. Modeling, 13, 465–486, 2006.

Fox, J. and Weisberg, S.: An R Companion to Applied Regression, SAGE Publications, 608 pp., ISBN 978-1-5443-3647-3, 2018.

Francis, E. J., Pourmohammadi, P., Steel, Z. L., Collins, B. M., and Hurteau, M. D.: Proportion of forest area burned at high-severity

increases with increasing forest cover and connectivity in western US watersheds, Landscape Ecol., 38, 2501–2518, 2023.

Galang, M. A., Markewitz, D., and Morris, L. A.: Soil phosphorus transformations under forest burning and laboratory heat treatments, Geoderma, 155, 401–408, 2010.

García-Oliva, F., Merino, A., Fonturbel, M. T., Omil, B., Fernández, C., and Vega, J. A.: Severe wildfire hinders renewal of soil P pools by thermal mineralization of organic P in forest soil: Analysis by sequential extraction and ^{31}P NMR spectroscopy, Geoderma, 309, 32–40, 2018.

Glaser, B., Lehmann, J., and Zech, W.: Ameliorating physical and chemical properties of highly weathered soils in the tropics with charcoal – a review, Biol. Fert. Soils, 35, 219–230, 2002.

Grieger, S., Bailey, J., Barnes, M., Bladon, K. D., Forbes, B., Garayburu-Caruso, V. A., Graham, E. B., Goldman, A. E., Homolka, K., McKever, S. A., Myers-Pigg, A., Otenburg, O., Renteria, L., Roebuck, A., Scheibe, T. D., and Torgeson, J. M.: Organic Matter Concentration and Composition of Experimentally Burned Open Air and Muffle Furnace Vegetation Chars across Differing Burn Severity and Feedstock Types from Pacific Northwest, USA (V3), ESS-Dive [data set], https://doi.org/10.15485/1894135, 2022.

Gundale, M. J. and DeLuca, T. H.: Temperature and source material influence ecological attributes of ponderosa pine and Douglas-fir charcoal, Forest Ecol. Manag., 231, 86–93, 2006.

Halofsky, J. E., Peterson, D. L., and Harvey, B. J.: Changing wildfire, changing forests: the effects of climate change on fire regimes and vegetation in the Pacific Northwest, USA, Fire Ecol., 16, 4, https://doi.org/10.1186/s42408-019-0062-8, 2020.

Hatch, L. E., Jen, C. N., Kreisberg, N. M., Selimovic, V., Yokelson, R. J., Stamatis, C., York, R. A., Foster, D., Stephens, S. L., Goldstein, A. H., and Barsanti, K. C.: Highly Speciated Measurements of Terpenoids Emitted from Laboratory and Mixed-Conifer Forest Prescribed Fires, Environ. Sci. Technol., 53, 9418–9428, 2019.

Haugo, R. D., Kellogg, B. S., Cansler, C. A., Kolden, C. A., Kemp, K. B., Robertson, J. C., Metlen, K. L., Vaillant, N. M., and Restaino, C. M.: The missing fire: quantifying human exclusion of wildfire in Pacific Northwest forests, USA, Ecosphere, 10, e02702, https://doi.org/10.1002/ecs2.2702, 2019.

Jolly, W. M., Cochrane, M. A., Freeborn, P. H., Holden, Z. A., Brown, T. J., Williamson, G. J., and Bowman, D. M. J. S.: Climate-induced variations in global wildfire danger from 1979 to 2013, Nat. Commun., 6, 7537, https://doi.org/10.1038/ncomms8537, 2015.

Keeley, J. E.: Fire intensity, fire severity and burn severity: a brief review and suggested usage, Int. J. Wildland Fire, 18, 116–126, 2009.

Kelly, S. D., Hesterberg, D., and Ravel, B.: Analysis of soils and minerals using X-ray absorption spectroscopy, in: Methods of Soil Analysis Part 5 – Mineralogical Methods, (Eds.) A. L. Ulery and L. R. Drees, American Society of Agronomy and Soil Science Society of America, Madison, WI, USA, 387–463, https://doi.org/10.2136/sssabookser5.5.c14, 2015.

Kruse, J., Abraham, M., Amelung, W., Baum, C., Bol, R., Kühn, O., Lewandowski, H., Niederberger, J., Oelmann, Y., Rüger, C., Santner, J., Siebers, M., Siebers, N., Spohn, M., Vestergren, J., Vogts, A., and Leinweber, P.: Innovative methods in soil phosphorus research: A review, J. Plant Nutr. Soil Sc., 178, 43–88, 2015.

Lane, P. N. J., Sheridan, G. J., Noske, P. J., and Sherwin, C. B.: Phosphorus and nitrogen exports from SE Australian forests following wildfire, J. Hydrol., 361, 186–198, 2008.

Lenth, R. V.: emmeans: Estimated marginal means, Github, https://doi.org/10.1080/00031305.1980.10483031, 2023.

Li, B. and Brett, M. T.: The influence of dissolved phosphorus molecular form on recalcitrance and bioavailability, Environ. Pollut., 182, 37–44, 2013.

Lopez, A. M., Avila, C. C. E., VanderRoest, J. P., Roth, H. K., Fendorf, S., and Borch, T.: Molecular insights and impacts of wildfire-induced soil chemical changes, Nature Reviews Earth & Environment, 5, 431–446, 2024.

Makarov, M. I., Haumaier, L., Zech, W., Marfenina, O. E., and Lysak, L. V.: Can ^{31}P NMR spectroscopy be used to indicate the origins of soil organic phosphates?, Soil Biol. Biochem., 37, 15–25, 2005.

McDowell, R. W., Worth, W., and Carrick, S.: Evidence for the leaching of dissolved organic phosphorus to depth, Sci. Total Environ., 755, 142392, https://doi.org/10.1016/j.scitotenv.2020.142392, 2021.

McMeeking, G. R., Kreidenweis, S. M., Baker, S., Carrico, C. M., Chow, J. C., Collett Jr., J. L., Hao, W. M., Holden, A. S., Kirchstetter, T. W., Malm, W. C., Moosmüller, H., Sullivan, A. P., and Wold, C. E.: Emissions of trace gases and aerosols during the open combustion of biomass in the laboratory, J. Geophys. Res. D-Atmos., 114, D19210, https://doi.org/10.1029/2009JD011836, 2009.

Merino, A., Jiménez, E., Fernández, C., Fontúrbel, M. T., Campo, J., and Vega, J. A.: Soil organic matter and phosphorus dynamics after low intensity prescribed burning in forests and shrubland, J. Environ. Manage., 234, 214–225, 2019.

Method 365.3: Phosphorus, All Forms (Colorimetric, Ascorbic Acid, Two Reagent): https://www.epa.gov/sites/default/files/2015-08/documents/method_365-3_1978.pdf (last access: July 2024), 1978.

Mishra, A., Alnahit, A., and Campbell, B.: Impact of land uses, drought, flood, wildfire, and cascading events on water quality and microbial communities: A review and analysis, J. Hydrol., 596, 125707, https://doi.org/10.1016/j.jhydrol.2020.125707, 2021.

Mukherjee, A. and Zimmerman, A. R.: Organic carbon and nutrient release from a range of laboratory-produced biochars and biochar–soil mixtures, Geoderma, 193–194, 122–130, 2013.

Myers-Pigg, A. N., Grieger, S., Roebuck Jr., J. A., Barnes, M. E., Bladon, K. D., Bailey, J. D., Barton, R., Chu, R. K., Graham, E. B., Homolka, K. K., Kew, W., Lipton, A. S., Scheibe, T., Toyoda, J. G., and Wagner, S.: Experimental Open Air Burning of Vegetation Enhances Organic Matter Chemical Heterogeneity Compared to Laboratory Burns, Environ. Sci. Technol., 58, 9679–9688, 2024.

Noack, S. R., McLaughlin, M. J., Smernik, R. J., McBeath, T. M., and Armstrong, R. D.: Crop residue phosphorus: speciation and potential bio-availability, Plant Soil, 359, 375–385, 2012.

Parsons, A., Robichaud, P., Lewis, S. A., Napper, C., and Clark, J. T.: Field guide for mapping post-fire soil burn severity, United States Department of Agriculture Forest Service Rocky Moun-

tain Research Station, https://doi.org/10.2737/RMRS-GTR-243, 2010.

R Core Team: R: A Language and Environment for Statistical Computing, 2023.

Randerson, J. T., Chen, Y., van der Werf, G. R., Rogers, B. M., and Morton, D. C.: Global burned area and biomass burning emissions from small fires, Biogeosciences, 117, G04012, https://doi.org/10.1029/2012JG002128, 2012.

Ravel, B. and Newville, M.: ATHENA, ARTEMIS, HEPHAESTUS: data analysis for X-ray absorption spectroscopy using IFEFFIT, J. Synchrotron Radiat., 12, 537–541, 2005.

Recena, R., Cade-Menun, B. J., and Delgado, A.: Organic phosphorus forms in agricultural soils under Mediterranean climate, Soil Sci. Soc. Am. J., 82, 783–795, 2018.

Reilly, M. J., Dunn, C. J., Meigs, G. W., Spies, T. A., Kennedy, R. E., Bailey, J. D., and Briggs, K.: Contemporary patterns of fire extent and severity in forests of the Pacific Northwest, USA (1985–2010), Ecosphere, 8, e01695, https://doi.org/10.1002/ecs2.1695, 2017.

Robinson, J. S., Baumann, K., Hu, Y., Hagemann, P., Kebelmann, L., and Leinweber, P.: Phosphorus transformations in plant-based and bio-waste materials induced by pyrolysis, Ambio, 47, 73–82, 2018.

Roebuck Jr., J. A., Grieger, S., Barnes, M. E., Gillespie, X., Bladon, K. D., Bailey, J. D., Graham, E. B., Chu, R., Kew, W., Scheibe, T. D., and Myers-Pigg, A. N.: Molecular shifts in dissolved organic matter along a burn severity continuum for common land cover types in the Pacific Northwest, USA, Sci. Total Environ., 958, 178040, https://doi.org/10.1016/j.scitotenv.2024.178040, 2024.

Rose, T. J., Schefe, C., Weng, Z., Rose, M. T., van Zwieten, L., Liu, L., and Rose, A. L.: Phosphorus speciation and bioavailability in diverse biochars, Plant Soil, 443, 233–244, 2019.

Rust, A. J., Hogue, T. S., Saxe, S., and McCray, J.: Post-fire water-quality response in the western United States, Int. J. Wildland Fire, 27, 203–216, https://doi.org/10.1071/WF17115, 2018.

Saa, A., Trasar-Cepeda, M. C., Gil-Sotres, F., and Carballas, T.: Changes in soil phosphorus and acid phosphatase activity immediately following forest fires, Soil Biol. Biochem., 25, 1223–1230, 1993.

Santín, C., Doerr, S. H., Merino, A., Bucheli, T. D., Bryant, R., Ascough, P., Gao, X., and Masiello, C. A.: Carbon sequestration potential and physicochemical properties differ between wildfire charcoals and slow-pyrolysis biochars, Sci. Rep., 7, 11233, https://doi.org/10.1038/s41598-017-10455-2, 2017.

Santín, C., Otero, X. L., Doerr, S. H., and Chafer, C. J.: Impact of a moderate/high-severity prescribed eucalypt forest fire on soil phosphorous stocks and partitioning, Sci. Total Environ., 621, 1103–1114, 2018.

Schaller, J., Tischer, A., Struyf, E., Bremer, M., Belmonte, D. U., and Potthast, K.: Fire enhances phosphorus availability in topsoils depending on binding properties, Ecology, 96, 1598–1606, 2015.

Silber, A., Levkovitch, I., and Graber, E. R.: pH-dependent mineral release and surface properties of cornstraw biochar: agronomic implications, Environ. Sci. Technol., 44, 9318–9323, 2010.

Silins, U., Bladon, K. D., Kelly, E. N., Esch, E., Spence, J. R., Stone, M., Emelko, M. B., Boon, S., Wagner, M. J., Williams, C. H. S., and Tichkowsky, I.: Five-year legacy of wildfire and salvage logging impacts on nutrient runoff and aquatic plant, invertebrate, and fish productivity, Ecohydrol., 7, 1508–1523, 2014.

Smil, V.: Phosphorus in the Environment: Natural Flows and Human Interferences, Annu. Rev. Env. Resour., 25, 53–88, 2000.

Son, J.-H., Kim, S., and Carlson, K. H.: Effects of Wildfire on River Water Quality and Riverbed Sediment Phosphorus, Water Air Soil Pollut. Focus, 226, 26, https://doi.org/10.1007/s11270-014-2269-2, 2015.

Souza-Alonso, P., Prats, S. A., Merino, A., Guiomar, N., Guijarro, M., and Madrigal, J.: Fire enhances changes in phosphorus (P) dynamics determining potential post-fire soil recovery in Mediterranean woodlands, Sci. Rep., 14, 21718, https://doi.org/10.1038/s41598-024-72361-8, 2024.

Stavi, I.: Wildfires in Grasslands and Shrublands: A Review of Impacts on Vegetation, Soil, Hydrology, and Geomorphology, Water, 11, 1042, https://doi.org/10.3390/w11051042, 2019.

Sun, K., Qiu, M., Han, L., Jin, J., Wang, Z., Pan, Z., and Xing, B.: Speciation of phosphorus in plant- and manure-derived biochars and its dissolution under various aqueous conditions, Sci. Total Environ., 634, 1300–1307, 2018.

Turner, B. L., Cade-Menun, B. J., and Westermann, D. T.: Organic Phosphorus Composition and Potential Bioavailability in Semi-Arid Arable Soils of the Western United States, Soil Sci. Soc. Am. J., 67, 1168–1179, 2003a.

Turner, B. L., Mahieu, N., and Condron, L. M.: Phosphorus-31 nuclear magnetic resonance spectral assignments of phosphorus compounds in soil NaOH–EDTA extracts, Soil Sci. Soc. Am. J., 67, 497–510, 2003b.

Turrion, M.-B., Lafuente, F., Aroca, M.-J., López, O., Mulas, R., and Ruipérez, C.: Characterization of soil phosphorus in a fire-affected forest Cambisol by chemical extractions and ^{31}P-NMR spectroscopy analysis, Sci. Total Environ., 408, 3342–3348, 2010.

Uchimiya, M. and Hiradate, S.: Pyrolysis temperature-dependent changes in dissolved phosphorus speciation of plant and manure biochars, J. Agr. Food Chem., 62, 1802–1809, 2014.

Uchimiya, M., Hiradate, S., and Antal Jr., M. J.: Dissolved Phosphorus Speciation of Flash Carbonization, Slow Pyrolysis, and Fast Pyrolysis Biochars, ACS Sustain. Chem. Eng., 3, 1642–1649, 2015.

Vega, J. A., Fontúrbel, T., Merino, A., Fernández, C., Ferreiro, A., and Jiménez, E.: Testing the ability of visual indicators of soil burn severity to reflect changes in soil chemical and microbial properties in pine forests and shrubland, Plant Soil, 369, 73–91, 2013.

Weihrauch, C. and Opp, C.: Ecologically relevant phosphorus pools in soils and their dynamics: The story so far, Geoderma, 325, 183–194, 2018.

Werner, F. and Prietzel, J.: Standard Protocol and Quality Assessment of Soil Phosphorus Speciation by P K-Edge XANES Spectroscopy, Environ. Sci. Technol., 49, 10521–10528, 2015.

Wu, H., Yip, K., Kong, Z., Li, C.-Z., Liu, D., Yu, Y., and Gao, X.: Removal and Recycling of Inherent Inorganic Nutrient Species in Mallee Biomass and Derived Biochars by Water Leaching, Ind. Eng. Chem. Res., 50, 12143–12151, 2011.

Wu, Y., Pae, L. M., Gu, C., and Huang, R.: Phosphorus Chemistry in Plant Ash: Examining the Variation across Plant Species and Compartments, ACS Earth Space Chem.,

https://doi.org/10.1021/acsearthspacechem.3c00145, 7, 2205–2013, 2023a.

Wu, Y., Pae, L. M., and Huang, R.: Phosphorus chemistry in plant charcoal: interplay between biomass composition and thermal condition, Int. J. Wildland Fire, 33, 2023b.

Xu, G., Zhang, Y., Shao, H., and Sun, J.: Pyrolysis temperature affects phosphorus transformation in biochar: Chemical fractionation and ^{31}P NMR analysis, Sci. Total Environ., 569–570, 65–72, 2016.

Yan, Y., Wan, B., Jiang, R., Wang, X., Wang, H., Lan, S., Zhang, Q., and Feng, X.: Interactions of organic phosphorus with soil minerals and the associated environmental impacts: A review, Pedosphere, 33, 74–92, 2023.

Yu, F., Wang, J., Wang, X., Wang, Y., Guo, Q., Wang, Z., Cui, X., Hu, Y., Yan, B., and Chen, G.: Phosphorus-enriched biochar from biogas residue of Eichhornia crassipes: transformation and release of phosphorus, Biochar, 5, 82, https://doi.org/10.1007/s42773-023-00281-3, 2023.

Yusiharni, E. and Gilkes, R.: Minerals in the ash of Australian native plants, Geoderma, 189–190, 369–380, 2012.

Zavala, L. M., De Celis, R., and Jordán, A.: How wildfires affect soil properties. A brief review, Cuad. Investig. Geogr., 40, 311–332, 2014.

Zheng, H., Wang, Z., Deng, X., Zhao, J., Luo, Y., Novak, J., Herbert, S., and Xing, B.: Characteristics and nutrient values of biochars produced from giant reed at different temperatures, Bioresource Technol., 130, 463–471, 2013.

Zwetsloot, M. J., Lehmann, J., and Solomon, D.: Recycling slaughterhouse waste into fertilizer: how do pyrolysis temperature and biomass additions affect phosphorus availability and chemistry?, J. Sci. Food Agr., 95, 281–288, 2015.